



Get Clarity On Generics

Cost-Effective CT & MRI Contrast Agents

 FRESENIUS
KABI

[WATCH VIDEO](#)

AJNR

The Success of Flow Diversion in Large and Giant Sidewall Aneurysms May Depend on the Size of the Defect in the Parent Artery

J.C. Gentric, T.E. Darsaut, A. Makoyeva, I. Salazkin and J. Raymond

This information is current as of August 10, 2025.

AJNR Am J Neuroradiol 2014, 35 (11) 2119-2124

doi: <https://doi.org/10.3174/ajnr.A4010>

<http://www.ajnr.org/content/35/11/2119>

The Success of Flow Diversion in Large and Giant Sidewall Aneurysms May Depend on the Size of the Defect in the Parent Artery

J.C. Gentric, T.E. Darsaut, A. Makoyeva, I. Salazkin, and J. Raymond

ABSTRACT

BACKGROUND AND PURPOSE: Flow diverters are designed to occlude aneurysms while preserving flow to jailed arterial branches. We postulated that treatment success depended on the size of the aneurysm ostium or defect in the parent artery.

MATERIALS AND METHODS: Flow diverter expansion and deformation were studied in silicone tubes with wall apertures of various sizes. Large and giant canine sidewall aneurysms, featuring a branch located immediately opposite the aneurysm, and a smaller 6- to 8-mm (group A, $n = 6$) or a larger 10- to 16-mm (group B, $n = 6$) ostium were created to study the effects of ostium size on aneurysm or branch occlusion by flow diverters. Angiographic results after deployment and at 3 months were scored by using an ordinal scale. The amount of neointima formation on the segment of the device overlying the aneurysm or the branch ostia was determined by specimen photography.

RESULTS: The fusiform deformation of flow diverters was maximal with larger defects in silicone tubes. At 3 months, group B aneurysms showed worse angiographic results than group A aneurysms, with larger residual aneurysm volumes ($P = .002$). Neointimal coverage of the aneurysm ostia was more complete in group A compared with group B ($P = .002$).

CONCLUSIONS: The effects of flow diversion may vary with the size of the aneurysm ostium.

ABBREVIATIONS: FD = flow diverter; FSS = free segment of the stent

Flow diverters are increasingly used to treat large, giant, and, more recently, bifurcation aneurysms.¹⁻⁸ Successful treatment of the aneurysm with a flow diverter (FD) requires protecting the patient from rupture by reducing aneurysm flow, promoting thrombosis, and perhaps even repairing the defect in the parent artery, without occluding arterial branches covered by the device. The optimal device porosity and pore density to successfully occlude aneurysms while sparing jailed branches remain unknown and most likely differ from case to case. While FDs have been introduced in the market as if 1 porosity would be appropriate for

all cases, previous studies, in a modular carotid aneurysm model, have shown that some FDs are capable of occluding straight sidewall aneurysms but fail when implanted across curved sidewall, bifurcation, or giant fusiform aneurysms with multiple side branches.⁹⁻¹²

The capacity for a particular FD to occlude an aneurysm may correlate with the size of the defect in the parent vessel or ostium of the aneurysm. In the present investigation, we explored how flow diverters become deformed in silicone tubes in which wall defects of variable sizes have been created. Deformation of the device may change its capacity to divert flow. In vivo, we used a straight sidewall aneurysm model, a configuration previously shown to be favorable to flow diversion,⁹ but modified to obtain large or giant aneurysms with variable-sized ostia (small or wide), to study how the size of the defect of the parent artery could influence device expansion, deformation, shortening, and angulation and how it could affect the efficacy of aneurysm occlusion at 3 months.

MATERIALS AND METHODS

The 3.75×32 mm FDs used were stent-in-stent constructions made of 1 outer high-porosity braided stent (similar to the LVIS; MicroVention, Tustin, California) and 1 inner low-porosity FD (a stent-in-stent construction similar to the FRED; MicroVention).

Received February 19, 2014; accepted after revision April 21.

From the Department of Radiology (J.C.G., J.R.), Centre Hospitalier de l'Université de Montréal, Notre-Dame Hospital, Montreal, Quebec, Canada; Groupe d'étude de la Thrombose en Bretagne Occidentale (J.C.G.), Université de Bretagne Occidentale, Brest, France; Division of Neurosurgery (T.E.D.), Department of Surgery, University of Alberta Hospital, Mackenzie Health Sciences Centre, Edmonton, Alberta, Canada; and Laboratory of Interventional Neuroradiology (A.M., I.S., J.R.), Centre Hospitalier de l'Université de Montréal, Notre-Dame Hospital Research Centre, Montreal, Quebec, Canada.

This work was supported by a grant from the Heart and Stroke Foundation of Alberta to Tim E. Darsaut.

Please address correspondence to Jean Raymond, MD, Centre Hospitalier de l'Université de Montréal, Notre-Dame Hospital, Interventional Neuroradiology, 1560 Sherbrooke East, Pavillion Simard, Room Z12909, Montreal, Quebec, Canada H2L 4M1; e-mail: jean.raymond@umontreal.ca

<http://dx.doi.org/10.3174/ajnr.A4010>

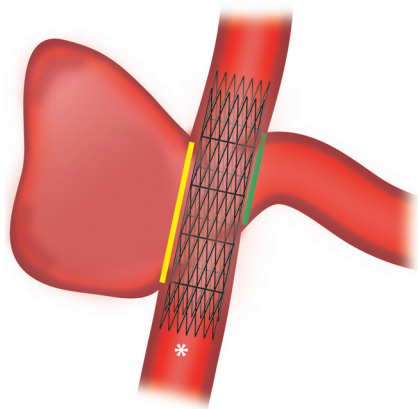


FIG 1. Description of the model. Schematic showing the branch opposite the constructed lateral wall aneurysm, with the proximal portion of the flow diverter denoted by an asterisk. Aneurysm-FSS is shown in yellow, and the branch-FSS is shown in green.

Benchtop experiments were performed by using FDs with inner stents of 36, 48, and 64 wires. All in vivo experiments were performed with devices characterized by a very low-porosity inner stent made of 64 braided wires. All devices were gifts from MicroVention.

Benchtop Studies

Experiments were performed by using silicone tubes of various diameters (2.0, 2.5, 3.5, 4.0 mm), simulating the parent carotid arteries of the animal model. We cut elliptic holes of various lengths (5, 10, 15 mm) from the tubes, removing a varied proportion of the tube circumference (approximately 25%, 50%, or 75%) for 9 different apertures. FDs were deployed within the silicone tubes by using standard deployment techniques. Microphotographs, scaled by including a ruler in the experimental setup, were taken for each condition with a stereomicroscope and were analyzed with image-processing software (ImageJ software; National Institutes of Health, Bethesda, Maryland).¹³ Given a sufficiently large opening, flow diverters progressively adopted a characteristic fusiform deformation,^{3,13} with 2 transition zones on each side of a compaction zone. Porosities of the transition zones were measured by calculating 1-metallic surface of the device.

In Vivo Studies

Surgical Construction of Aneurysms. All procedures were performed in 7- to 10-kg beagles under general anesthesia, in accordance with the guidelines of the Canadian Council on Animal Care. The model used is a modification of the one previously described (Fig 1).⁹

Briefly, through a linear midline incision, a segment (>30 mm) of the external jugular vein was harvested; then the pretracheal fascia was incised to expose and gain access to both carotid arteries. Under flow arrest, we ligated the left carotid artery proximally and tunneled the distal end behind the esophagus, anastomosing the left carotid to the right carotid artery in an end-to-side configuration. To create giant aneurysms, we anastomosed the venous segment to the right carotid artery side-to-side on the arterial wall.⁹ The arteriotomy on the right carotid artery was short (between 6 and 8 mm, group A; $n = 6$) or long (between 10

and 16 mm, group B; $n = 6$) to receive the side-to-side venous graft and produce ostia of various sizes. All incisions were closed in multiple layers (Fig 1).

Endovascular Treatment and Angiography. Four days before endovascular treatment, animals were premedicated with acetyl salicylic acid, 81 mg daily, along with a loading dose of 150 mg of clopidogrel, followed by 37.5 mg daily. Endovascular treatment was performed 4–6 weeks after surgical aneurysm construction, through a coaxial microcatheter system introduced by a percutaneous transfemoral approach. All aneurysms were treated with a single 64-wire FD, deployed to leave a minimum of approximately 10-mm landing zones on each side. Clopidogrel therapy was discontinued 10 days post-stent implantation, while acetyl salicylic acid, 81 mg per day, was continued until euthanasia. Transfemoral angiography was performed in all animals immediately before and following FD deployment, at 2 weeks, and immediately before euthanasia at 3 months. To prevent femoral hematomas on dual antiplatelet therapy, all punctured femoral arteries were surgically exposed through a small linear incision and ligated. Angiographic results were scored by 2 experienced observers (T.E.D. and J.R.) by using a previously published system modified from Kamran et al.¹ A score of 0 indicated no change in aneurysm volume with treatment; 1, residual contrast filling >50% of the pretreatment aneurysm volume; 2, residual contrast filling <50% of the pretreatment aneurysm volume; 3, residual filling confined to the neck region; and 4, no residual filling (complete occlusion). The length and width of residual aneurysms at 3 months were also measured by using the distal tip of the angiographic catheter as a fiducial marker to calibrate measurements. The fusiform deformation of the device was measured by the ratio of the diameter of the device at the level of the midpoint of the ostium divided by the mean diameter of the device measured proximal and distal to the ostial opening of aneurysms. The angle between the proximal and distal carotid artery segments of the devices was also measured in the coronal plane defined by the 2 anastomoses, by drawing lines in the center of the lumen of the carotid arteries. The patency of the parent arteries and arterial branches was also assessed, and stenoses, if present, were calculated by using $1 - N / D$, where N indicates the diameter at the level of the more severe stenosis and D , the diameter of the distal normal artery.

Euthanasia and Pathology. Euthanasia by barbiturate overdose was performed at 3 months. After fixation in 10% formalin, the carotid artery aneurysm construct was opened longitudinally. We studied the portion of the stent that was visible over the aneurysm ostium. This free segment of the stent (FSS) or aneurysm-FSS,¹⁴ was photographed by using a computerized imaging system (Vision PE; Clemex Technologies, Longueuil, Quebec, Canada). We also attempted to separately assess the branch-FSS, the segment of the FD covering the ostium of the left carotid artery (Fig 1). For each ex vivo aneurysm and branch, we attempted to determine the final porosity (the surface area through which blood could flow after neointima formation on the FSS), which was calculated by taking 1 minus the surface area of the biologic material plus the area of the metal struts, divided by the ostial surface area, as described by Bing et al.¹² Neointimal coverage was graded by 2 ex-

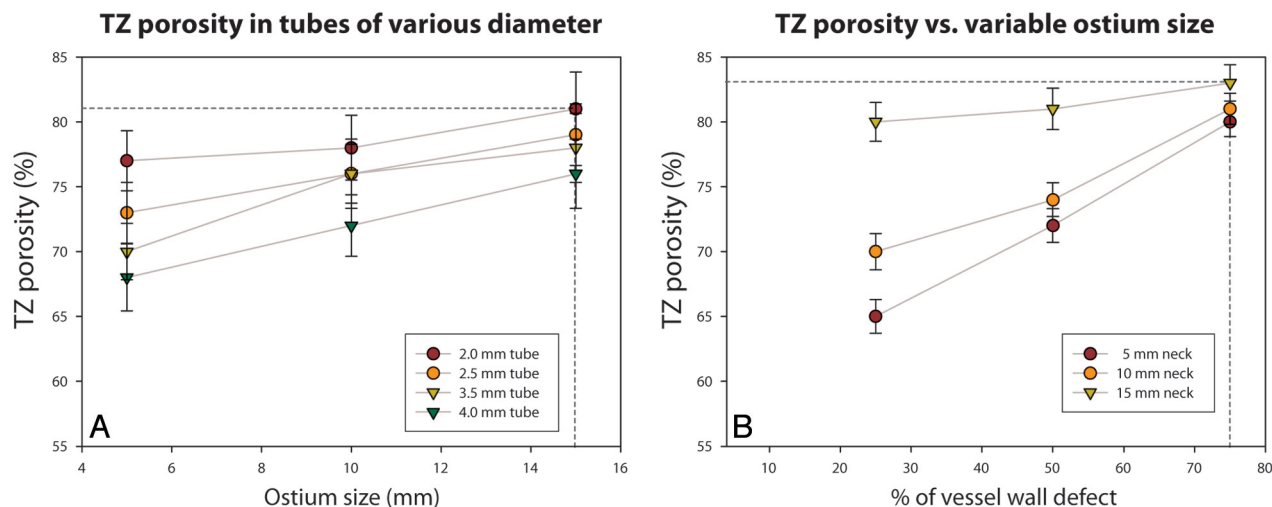


FIG 2. Result of benchtop studies. The porosity of the transition zones (TZs) is shown to increase when FDs are constrained in tubes of smaller diameters (A), when the size of the defect is increased in length (A), or when the opening takes a greater proportion of the silicone tube circumference (B).

Aneurysm characteristics and evolution with treatment

Animal	Initial Aneurysm Dimensions		Final Aneurysm Dimensions (L × W) (mm)	Neointima Formation on FD (%)		Arterial Stenoses (%)		Angiographic Score	Device Geometry	
	Ostium (mm)	Fundus (L × W) (mm)		Aneurysm FSS	Branch FSS	Stented Artery	Jailed Artery		Ratio of Fusiform Dilation	Angle
Group A										
1	8	30 × 10	16 × 5	90	20	50	0	2	1.8	6°
2	7	15 × 10	9 × 4	80	90	40	20	2	1.6	9°
3	8	35 × 10	13 × 10	80	80	20	0	2	1.8	5°
4	8	26 × 10	9 × 16	90	80	20	50	2	2.5	4°
5	8	17 × 7	17 × 9	70	80	50	0	2	1.4	−6°
6	6	17 × 7	4 × 3	100	80	50	0	3	1.5	−6°
Group B										
7	16	34 × 10	42 × 12	10	0	10	0	0	1.3	30°
8	14	28 × 8	39 × 8	50	60	10	80	0	1.5	26°
9	15	35 × 8	39 × 8	50	80	50	0	0	2.5	26°
10	14	32 × 7	35 × 11	50	50	50	30	0	2.2	25°
11	10	24 × 7	35 × 11	60	90	40	0	0	1.5	16°
12	11	30 × 10	39 × 11	50	90	20	0	0	1.7	16°

Note:—L × W indicates length × width.

perienced observers (I.S. and J.R.), and disagreements were resolved during a consensus session. Selected samples of tissue coverage over areas of interest were biopsied under a microscope. Biopsy specimens were stained with hematoxylin-eosin and Movat Pentachrome, followed by immunohistochemistry with smooth-muscle cell α -actin and endothelial Factor VIII.

Statistics

Comparisons between groups were made by using the Mann-Whitney test for nonparametric data. For paired data, the Wilcoxon signed rank test was used instead. Correlations between nonparametric data were explored with Spearman rank correlation coefficient ρ . All analyses were carried out with SPSS, Version 20 (IBM, Armonk, New York).

RESULTS

Benchtop Studies

When constrained within silicone tubes smaller than their diameter, all types of FDs tend to expand through the defect in the wall

of the tube, provided the defect is sufficiently large. This expansion causes a fusiform deformation, associated with a characteristic pattern of changing porosities, with a middle compaction zone between 2 transition zones. The transition zones are more porous than the compaction zone, and the porosity of the transition zone increases as the defect in the parent vessel increases in length (Fig 2A), as the defect takes a larger proportion of the wall circumference (Fig 2B), and with a larger discrepancy between tube diameter and the diameter of the stent (Fig 2A). The porosity of the transition zone is maximal, with a combination of the smallest parent vessel diameter with the longest and largest circumferential wall defect (Fig 2B).

In Vivo Results

The aneurysm characteristics and evolution with treatment are summarized in the Table and illustrated in Fig 3.

Group B aneurysms had significantly wider ostia (mean, 13 ± 2 mm) than group A aneurysms (8 ± 1 mm; $P = .002$), but other

aneurysm dimensions and volumes were similar before treatment ($P = .7$).

At 3 months, wider ostium aneurysms had significantly worse angiographic outcomes (median Kamran score of 0) than smaller ostium aneurysms (median score of 2; $P = .002$).

Aneurysm volumes were also significantly different at 3 months (mean, $16,915 \pm 5724 \text{ mm}^3$ compared with $2500 \pm 2468 \text{ mm}^3$; $P = .002$); while smaller ostium aneurysms had substantially decreased in size (mean, $-6063 \pm 4949 \text{ mm}^3$), wider ostium aneurysms had increased in size at 3 months (mean, $+7717 \pm 4826 \text{ mm}^3$; $P = .004$).

Neointimal coverage of the aneurysm-FSS was more complete in the smaller ostium (mean, $85 \pm 10\%$) compared with the wider ostium aneurysms (mean, $45 \pm 18\%$; $P = .002$). There was no significant difference between neointimal coverage of the aneurysm or branch-FSS ($P = .57$) and no difference in branch-FSS neointimal coverage between groups ($P = .82$).

A fusiform deformation of devices was observed at the level of the aneurysm ostium in most cases but was of similar extent in both groups (mean ratio of diameters, 1.8 ± 0.5 ; $P = .82$). The angle between the proximal and distal halves of the device within the parent artery was significantly different in wider ostium ($23 \pm 6^\circ$) compared with smaller ostium aneurysms ($2 \pm 6^\circ$; $P = .002$).

There was no significant difference in the degree of parent artery or branch stenosis between groups.

The most significant correlation was found between neointimal coverage of the aneurysm-FSS and angiographic evolution of aneurysms ($\rho = -0.757$, $P = .004$). There was also a significant correlation between the angiographic evolution of lesions at 3 months and the size of the ostium ($\rho = 0.620$, $P = .03$). Angiographic evolution nearly significantly correlated with parent vessel angle ($\rho = 0.573$, $P = .05$), but no significant correlation was found with the extent of fusiform deformation of the device ($\rho = -0.424$, $P = .17$).

Pathologically, the smaller ostium aneurysms that decreased in size were partially filled with thrombus in various stages of organization combined with vascularized connective tissue, while wider ostium aneurysms were mostly empty and thick-walled. The portion of the device covering the aneurysm ostium (the aneurysm-FSS) was most often covered with thick mature neointima on both the aneurysm and parent artery surfaces, leaving visible holes within the metal struts, which were occasionally partially covered with unorganized thrombus where leaks presumably occurred. Sometimes the aneurysm was fed mainly by a major leak in the distal transition zone of the aneurysm-FSS, while the branch was fed mainly by a leak in the proximal transition zone of the branch-FSS (Fig 4). In some other cases, leaks could be detected at the distal margin of the inner stent, barely bridging the aneurysm ostium and not incorporated into the neointima that covered the landing zone of the outer stent (Fig 5). There was no difference in the appearance of the neointima covering the aneurysm or branch-FSS (Fig 3). Many branches appeared almost completely occluded by neointima at pathology, while no stenosis was perceptible by angiography performed immediately before euthanasia.

DISCUSSION

The main finding of this work is that the size of the arterial defect (or aneurysm ostium) was an important determinant of the evolution of aneurysms after flow diversion of large or giant sidewall aneurysms. The size of the defect can impact the fusiform deformation of the device and the porosity of the transition zones, at least in benchtop studies. While it is tempting to suggest that worse angiographic outcomes may be the result of the more extensive fusiform deformation seen with the in vitro studies that occurs when the aneurysm ostium is larger, there are other plausible variables to consider. The size of the ostium was also related to device protrusion and angulation, 2 factors that may impact flow diversion. Smaller ostium aneurysms had better neointimal coverage of the FSS and better angiographic evolution, compared with wider ostium large or giant aneurysms. Finally, branches that were bridged by the device were always patent, but substantial neointimal occlusion could also be found at the level of the branch-FSS.

While the sidewall aneurysm model was previously shown to be curable by flow diversion when the neck of aneurysms was small (approximately 5 mm),⁹ flow diversion can fail, even in this sidewall configuration, when the defect of the parent artery is large and the aneurysm is large or giant. Many potential mechanisms may contribute to the failure of flow diversion in this wide-ostium aneurysm model. The benchtop studies we performed showed that flow diverters cannot display the characteristic fusiform deformation they adopt when they are free to expand, unless the aperture in the parent vessel is long enough and takes up a sufficient enough proportion of the tube circumference to allow expansion and protrusion of the device through the ostium.^{12,13} In vivo, devices adopted the characteristic fusiform deformation as they crossed the level of the aneurysm ostium, but the deformation, when measured as a ratio of diameters, was not shown to be more substantial with wider aneurysm ostia, probably because even the smaller ostium aneurysms already had ostia sufficiently large for the deformation to be equally present in both groups (Table). The evolution of aneurysm size at follow-up correlated with neointimal coverage of the aneurysm-FSS, shown to be less complete in wide-ostium aneurysms.

Residual aneurysms were associated with leaks through the gaps in the neointima that tended to occur at the more porous transition zones. Asymmetric device protrusion through the ostium, with the development of an angle between the proximal and distal segments of the device, was constantly observed in the wider ostium aneurysms, and the angle correlated with angiographic evolution, with $\rho = 0.573$ and $P = .05$. This angle was shown in other studies to influence flow after stent placement and flow diversion in computational fluid dynamics studies and in vitro.² We speculate that this angle could perhaps have favored residual flow through the distal transition zone, which was always lacking neointimal coverage when aneurysms persisted at 3 months. Microscopically, leaks were found not only at the level of gaps in the neointima that covered the FSS but also beyond the distal margin of the inner stent, which shortened with expansion at the level of wider ostium aneurysms and may no longer have assured complete neointimal closure of the distal ostium (Fig 5). This phenomenon occurred despite the outer stent, the most visible por-

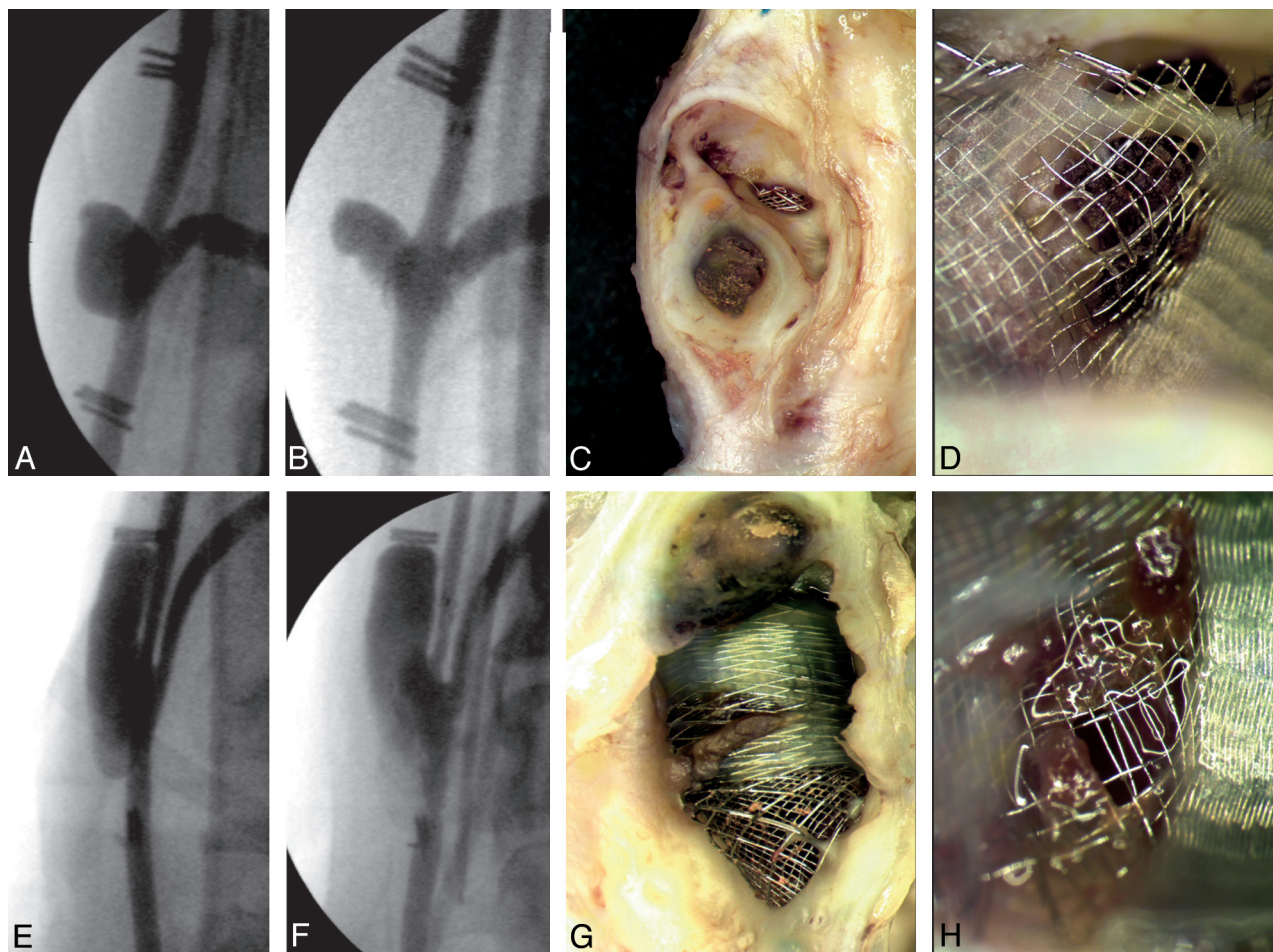


FIG 3. Results of in vivo studies. Initial preimplantation angiography (A and E), angiographic results at 3 months (B and F), and photographs of neointimal formation over the device at the level of the aneurysm- (C and G) or branch-FSS (D and H). Panels show how giant aneurysms with smaller ostia (A–D) are more completely occluded at 3 months, with more complete neointimal coverage of the aneurysm-FSS, than aneurysms with a wider ostium (E–H). Note how leaks are related to the more porous transition zones. Neointima formation over the branches is also substantial (D and H).

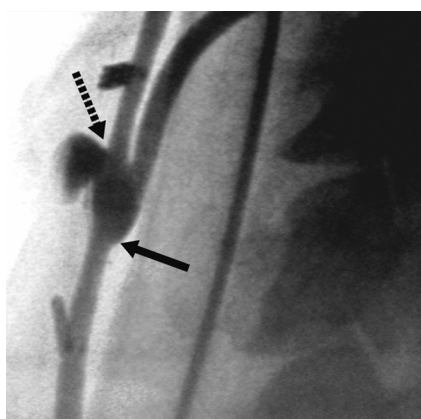


FIG 4. Transition zones and flows. Angiographic results 3 months after flow diversion show how the aneurysm fills from persistent flow through the distal transition zone (*dotted arrow*), while the branch is fed by the proximal transition zone (*arrow*).

tion of the device, being satisfactorily deployed with comfortable landing zones.

We speculate that device deformation, expansion, shortening, and angulation, responsible for treatment failures in this wide-

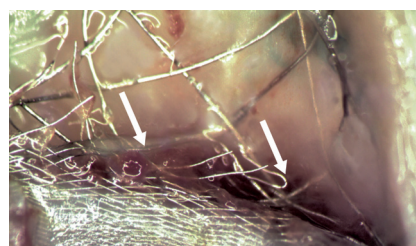


FIG 5. Distal ostial leaks. With device expansion in front of wider ostium aneurysms, there is deformation and shortening of the inner stent, which may no longer fully cover the distal edge of the aneurysm ostium (*arrows*).

ostium animal model, could theoretically be minimized by coiling the aneurysm sac or by stent placement before flow diversion. Because the devices we used were already stent-in-stent constructions, more rigid or stronger high-porosity stents would perhaps be necessary for this strategy to succeed.

The 64-wire devices we used for this study were of much lower porosity than the 36-wire devices that were shown to successfully treat sidewall aneurysms with even smaller (≈ 5 mm) necks.⁹ They are also less porous than clinically available 48-wire flow diverters. Therefore, we question whether the problems described here

could be completely solved by using devices of even lower porosities without jeopardizing the patency of branches or perforators or even of the parent vessel.

When this canine model was developed, we had postulated that neointima formation on the free segment of stent overlying the aneurysm ostium (or aneurysm-FSS) could meaningfully be compared with neointima formation overlying the branch ostium (the branch-FSS). Quantification of neointimal coverage of the aneurysm or branch-FSS, the segments of the device directly en face the aneurysm or branch ostium, did not turn out to be simple, and the meaning of the proportion of the segment of the device that was covered with neointima may not be as clear as hoped; sometimes large residual aneurysms persisted with only a small hole in the neointimal layer. When we carefully studied and correlated angiographic and pathologic specimens, we realized that blood flow can escape the flow diverter proximally, at the level of the proximal transition zone for example, and contribute to feeding the arterial branch. Thus, thick neointima formation at the level of the branch or aneurysm-FSS may be related to blood flowing inside and outside the lumen of the flow diverter, and neointimal gaps shown directly in front of the branch or aneurysm ostium may not represent all of the flow contributions to the branch or aneurysm.^{9,14}

Furthermore, the neointimal gaps we observed were not always in the center of the transition zone, which might have suggested, if neointima formation is centripetal, that the worse outcomes observed in the larger ostium aneurysms could have been related to the amount of time it takes for neointima to cover an implanted device. Because the neointimal gaps were observed to be heterogeneously distributed, we do not think that the failures occurred simply due to an insufficient length of time for the larger aneurysm ostia to be covered.

Limitations

The construction of large aneurysms with small ostia may result in smaller-sized aneurysms at the time of device implantation compared with aneurysms with larger ostia, as suggested by the seminal work of German and Black,¹⁵ though differences in initial aneurysm dimensions were not significant in the present work ($P = .7$). Whether the canine aneurysm models we have used can help predict the clinical efficacy of flow diverters in patients remains to be validated. The number of animals studied in this work is small, and long-term follow-up angiography beyond 3 months was not performed. We have previously shown, however, that failures at 3 months were not followed by improvement at 6 months.¹⁰ Experimental aneurysms were surgical constructions, with venous pouches anastomosed to cervical carotid arteries; hence, results may differ significantly from spontaneous intracranial aneurysms. Canine biology certainly differs from human biology, and any extrapolation of findings to clinical cases should remain cautious. Although the experimental canine model used here yields different results from those reported in clinical series, we, nonetheless, find them useful because more can be learned from failures than from success.

Finally, the FDs used in this work were prototypes, and substantial modifications of device construction and characteristics have since been made. The results we obtained may not apply to

devices currently available. The device deformations shown in benchtop studies have, however, been reproduced with the Pipeline Embolization Device (Covidien, Irvine, California).³

CONCLUSIONS

Flow diverters may fail to occlude large or giant sidewall aneurysms when the arterial defect or aneurysm ostium is too large. This failure may be related to device deformation and protrusion through the ostial opening and incomplete neointimal closure of the aneurysm ostium.

Disclosures: Tim E. Darsaut—*RELATED*: grant funding in direct support of the current work,* from the Heart and Stroke Foundation of Alberta (Protocol 678/01/13/D, funding agency/sponsor: Heart and Stroke Foundation, Research Service Office Project RES0011612). Tim E. Darsaut and Jean Raymond—*UNRELATED*: Canadian Institutes of Health Research operating grant unrelated (MOP-119554: for the Canadian Unruptured Endovascular versus Surgery (CURES) Trial [randomized controlled trial]).*
*Money paid to the institution.

REFERENCES

1. Kamran M, Yarnold J, Grunwald IQ, et al. **Assessment of angiographic outcomes after flow diversion treatment of intracranial aneurysms: a new grading schema.** *Neuroradiology* 2011;53:501–08
2. D'Urso PI, Lanzino G, Cloft HJ, et al. **Flow diversion for intracranial aneurysms: a review.** *Stroke* 2011;42:2363–68
3. Shapiro M, Raz E, Becske T, et al. **Variable porosity of the Pipeline embolization device in straight and curved vessels: a guide for optimal deployment strategy.** *AJNR Am J Neuroradiol* 2014;35:727–33
4. Pistocchi S, Blanc R, Bartolini B, et al. **Flow diverters at and beyond the level of the circle of Willis for the treatment of intracranial aneurysms.** *Stroke* 2012;43:1032–38
5. Becske T, Kallmes DF, Saatci I, et al. **Pipeline for uncoilable or failed aneurysms: results from a multicenter clinical trial.** *Radiology* 2013;267:858–68
6. Szikora I, Berentei Z, Kulcsar Z, et al. **Treatment of intracranial aneurysms by functional reconstruction of the parent artery: the Budapest experience with the Pipeline embolization device.** *AJNR Am J Neuroradiol* 2010;31:1139–47
7. Byrne J V, Beltechi R, Yarnold JA, et al. **Early experience in the treatment of intra-cranial aneurysms by endovascular flow diversion: a multicentre prospective study.** *PLoS One* 2010;5:9–8
8. Piano M, Valvassori L, Quilici L, et al. **Midterm and long-term follow-up of cerebral aneurysms treated with flow diverter devices: a single-center experience.** *J Neurosurg* 2013;118:408–16
9. Darsaut TE, Bing F, Salazkin I, et al. **Flow diverters can occlude aneurysms and preserve arterial branches: a new experimental model.** *AJNR Am J Neuroradiol* 2012;33:2004–09
10. Darsaut TE, Bing F, Salazkin I, et al. **Flow diverters failing to occlude experimental bifurcation or curved sidewall aneurysms: an in vivo study in canines.** *J Neurosurg* 2012;117:37–44
11. Darsaut TE, Bing F, Salazkin I, et al. **Testing flow diverters in giant fusiform aneurysms: a new experimental model can show leaks responsible for failures.** *AJNR Am J Neuroradiol* 2011;32:2175–79
12. Bing F, Darsaut TE, Salazkin I, et al. **Stents and flow diverters in the treatment of aneurysms: device deformation in vivo may alter porosity and impact efficacy.** *Neuroradiology* 2013;55:85–92
13. Makoyeva A, Bing F, Darsaut TE, et al. **The varying porosity of braided self-expanding stents and flow diverters: an experimental study.** *AJNR Am J Neuroradiol* 2013;34:596–602
14. Darsaut TE, Bing F, Makoyeva A, et al. **Flow diversion to treat aneurysms: the free segment of stent.** *J Neurointerv Surg* 2013; 5:452–57
15. German WJ, Black SP. **Experimental production of carotid aneurysms.** *N Engl J Med* 1954;250:104–06